IOP PUBLISHING EUROPEAN JOURNAL OF PHYSICS

Eur. J. Phys. **29** (2008) 215–233 doi:10.1088/0143-0807/29/2/005

Extraordinary oscillations of an ordinary forced pendulum

Eugene I Butikov

St Petersburg State University, St Petersburg, Russia

E-mail: butikov@EB12514.spb.edu

Received 16 October 2007, in final form 13 December 2007
Published 17 January 2008
Online at stacks.iop.org/EJP/29/215

Abstract

Several well-known and newly discovered counterintuitive regular and chaotic modes of the sinusoidally driven rigid planar pendulum are discussed and illustrated by computer simulations. The software supporting the investigation offers many interesting predefined examples that demonstrate various peculiarities of this famous physical model. Plausible physical explanations are suggested for some exotic and unexpected motions. This paper can be useful for graduate and advanced undergraduate students and their instructors. The suggested simulation program can also serve as an exploration-oriented tool for discovering new features of the driven pendulum and gives students an opportunity to perform mini-research projects on their own.

1. Introduction: the investigated physical system

If we ask ourselves which is the most famous instrument in the history of physics, our first idea may be about the pendulum. We may expect that an ordinary pendulum subjected to periodic forcing will exhibit quite familiar behaviour which agrees well with our intuition. However, despite the apparent simplicity, this well-known nonlinear system can display a rich variety of rather complex, as-yet-unexplored modes of motion which include various kinds of transient processes, single- and multiple-period stationary oscillations and complete revolutions, subharmonic and superharmonic resonance responses, bistability and multistability, intermittency, transient and stationary chaos. Most of these modes delight the eye and certainly challenge our physical intuition. By slowly varying the control parameters of the system (the frequency and amplitude of the drive, and damping factor), we can observe various kinds of bifurcations manifesting transitions of the pendulum between dramatically different modes of behaviour.

The seemingly simple situation of the forced pendulum occurred to be quite complex due to the subtle interplay between natural modes of the pendulum (these modes are described in detail in [1]) and the periodic driving force. The driven pendulum is interesting not only by

its role in the history of physics, but also, maybe more importantly, because it is isomorphic to many other physical systems including rf-driven Josephson junctions and phase-locked voltage-controlled oscillators. The equation of motion of the dissipative, externally driven pendulum serves as a paradigmatic model of various low-dimensional nonlinear dynamical systems and plays an important role in explorations of bifurcational and chaotic phenomena. Mechanical analogues of such systems allow us to observe a direct visualization of their motion and thus can be very useful in gaining an intuitive understanding of complex phenomena.

Numerous nonlinear problems in relation to the forced pendulum are clearly presented in [2]. The nonlinear phenomena that can be predicted by analytical methods are described in [3]. Detailed reviews of the experimental and theoretical investigations of various regular and chaotic features of the system are available in the literature (see, for example, [4, 5] and references therein).

An obvious way to understand the behaviour of a nonlinear mechanical system is to observe a computer simulation of its motion. Sometimes the simulations can tell us much more than the equations and thus contribute greatly in building our physical intuition. For this purpose, we have developed an educational interactive simulation program 'rigid pendulum driven by a sinusoidal torque' included in the package 'nonlinear oscillations' [6] available on the web. The software runs under the Windows operating system, and is accompanied by detailed instructions on its usage. The program illustrates the motion of the sinusoidally driven pendulum simulating all known modes of behaviour, and can also serve as a convenient tool for discovering new features of this seemingly inexhaustible system. Several known and new modes are described and explained in this paper, which can be useful for graduate and advanced undergraduate students and their instructors.

2. The physical model

In this paper and in the simulation program [6] we consider an ordinary planar rigid pendulum, say, a weightless rigid rod with a massive bob (point mass) at one end (a simple or mathematical pendulum), or any other massive body (a physical pendulum) that can turn about a horizontal axis in a uniform gravitational field. Being excited, the pendulum can rotate in the vertical plane or swing about the stable equilibrium position in which its centre of mass is below the axis. The period T_0 of infinitely small natural oscillations in the absence of friction is characteristic of the given pendulum and can serve as a convenient unit of time for the simulation. Natural oscillations gradually dampen due to friction whose braking torque is assumed in the model to be proportional to the angular velocity of the pendulum (viscous friction).

The momentary mechanical state of the pendulum is determined by its angular position φ, which is the angle of deflection from the vertical equilibrium position measured in radians (or degrees), and by the angular velocity $\dot{\varphi} = \mathrm{d}\varphi/\mathrm{d}t$ measured in the simulation program in units of the natural angular frequency ω_0 of (undamped) infinitely small oscillations of the pendulum ($\omega_0 = 2\pi/T_0$). We assume that the pendulum is directly driven by an external sinusoidal torque with the frequency ω and some constant amplitude.

The differential equation of motion used here and in the program [6] to simulate the damped driven pendulum is of the form

$$\ddot{\varphi} + 2\gamma\dot{\varphi} + \omega_0^2 \sin\varphi = \omega_0^2\phi_0 \sin\omega t. \tag{1}$$

Here, ω is the driving frequency and γ is the damping factor. To measure the viscous damping, we can use instead of γ a more convenient dimensionless quantity Q—the quality factor that equals the ratio $\omega_0/2\gamma$.

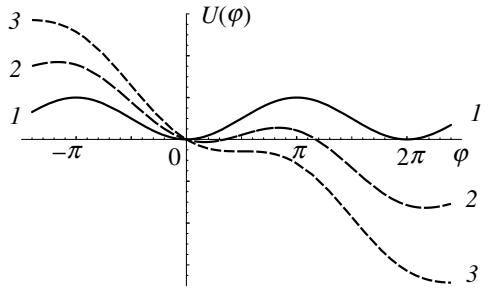

Figure 1. Potential energy $U(\varphi) \sim (1 - \cos\varphi - \phi\varphi)$ of the pendulum subjected to a static torque ϕ. Curve 1—$\phi = 0$, curve 2—$\phi = 0.5$, curve 3—$\phi = 1$.

The driving torque in the right-hand part of equation (1) is proportional to $\phi(t) = \phi_0 \sin\omega t$. This means that the dimensionless quantity $\phi(t)$ can be used as a convenient measure of the external torque. Its physical sense can be explained as follows. Imagine that some small constant (time-independent) external torque ϕ is exerted on the pendulum (instead of $\phi(t) = \phi_0 \sin\omega t$). This torque ϕ causes a static displacement φ of the pendulum from the vertical. The sine of this angular displacement is proportional to the torque. Indeed, for the pendulum in equilibrium the time derivatives of φ vanish ($\ddot{\varphi} = 0$ and $\dot{\varphi} = 0$), and we conclude from equation (1) that under a static torque ϕ the relation $\sin\varphi = \phi$ is valid. Hence $\phi = 1$ corresponds to the external torque necessary to hold the pendulum stationary at a horizontal position $\varphi = \pi/2$, the position of maximum restoring torque of gravity.

For small enough values of torques the displacement is small ($\varphi \ll 1$), and we can assume $\sin\varphi \approx \varphi$. That is, $\varphi \approx \phi$. This means that the angular displacement of the pendulum under a small static torque just equals this torque measured in the assumed angular units. In the limit of a very low driving frequency (when $\omega \to 0$) the pendulum adiabatically follows the external torque, and the low-frequency steady-state forced oscillation of the pendulum will occur just with the amplitude of the driving torque measured in these units (provided the amplitude is small enough so that the static displacement is proportional to the torque).

3. Behaviour of the pendulum under the slow varying sinusoidal torque whose amplitude $\phi_0 \approx 1$

Graphs of potential energy $U(\varphi) \sim (1 - \cos\varphi - \phi\varphi)$ for the pendulum subjected to a static torque ϕ are shown in figure 1 for several values of ϕ. In the absence of external torque ($\phi = 0$) stable equilibrium positions—minima of $U(\varphi)$—are located at $\varphi = \pm 2\pi n, n = 0, 1, \ldots$. Natural oscillations of the down-hanging pendulum can occur in any of the equivalent potential wells (say, about the midpoint $\varphi = 0$) with the frequency ω_0. The static torque ϕ causes a displacement of the equilibrium position to $\varphi = \arcsin\phi$. The pendulum can be in equilibrium under a static torque if $\phi < 1$ (curves 1 and 2 in figure 1); at greater values of ϕ potential energy $U(\varphi)$ has no minima (curve 3 in figure 1) so that equilibrium (as well as an oscillatory motion) is impossible: the pendulum rotates. When $\phi \to 1$, the static displacement $\varphi \to \pi/2$ (tends to the horizontal position of the pendulum).

The case of a slow varying sinusoidal torque whose amplitude $\phi_0 \approx 1$ deserves special investigation. Figure 2 shows the time-dependent graph of the steady-state motion at $\omega = 0.01\omega_0$ under the driving torque whose amplitude ϕ_0 slightly exceeds one radian. Period

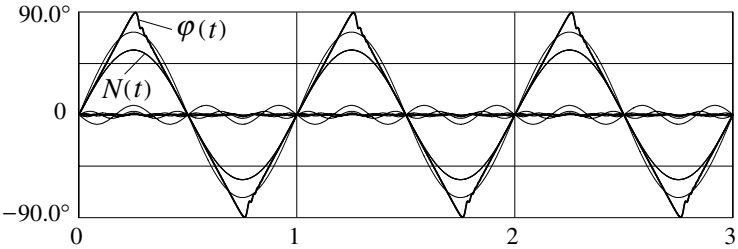

(quality 10.0, driving freq. 0.01, driving ampl. 57.2958, initial defl. 0.0558 degr., init. ang. velocity 0.01)

Figure 2. Steady-state motion of the pendulum at $\phi_0 \approx 1$ under sinusoidal torque $N(t)$ of a low driving frequency ($\omega = 0.01\omega_0$). Harmonic components of $\varphi(t)$ are also shown.

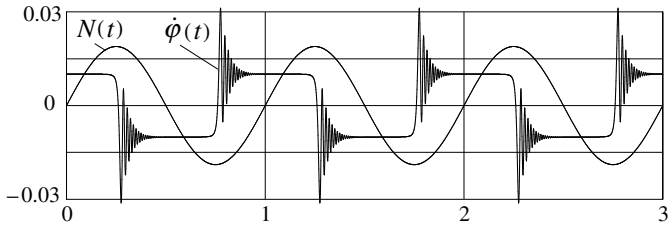

Figure 3. Angular velocity at the low-frequency ($\omega = 0.01\omega_0$) motion of the pendulum under the sinusoidal torque $N(t)$ whose amplitude $\phi_0 \approx 1$.

$T = 2\pi/\omega$ of the driving torque is chosen in this graph as an appropriate time unit. We note a linear dependence of $\varphi(t)$ on time when the external torque $N(t)$ increases sinusoidally from zero to its maximal value $\phi_0 = 1$.

Next we try to explain this counterintuitive behaviour of the pendulum on the basis of the differential equation (1). For a slow steady-state motion (at $\omega \ll \omega_0$), we can ignore the terms with the angular velocity and acceleration in the differential equation (1) of the pendulum. In other words, the pendulum adiabatically follows the slow-varying external torque remaining in the equilibrium position all the time (in the potential energy minimum), which is displaced from the vertical by the external torque. The sine of this angular displacement $\varphi(t)$ is equal to the torque $\phi(t) = \phi_0 \sin\omega t$. This is evident from equation (1). Therefore for $\phi_0 = 1$ we get $\sin\varphi(t) = \sin\omega t$, and hence for the time interval $(0, T/4)$ the angle of deflection $\varphi(t) = \omega t$: when the external torque $\phi(t)$ increases sinusoidally, the equilibrium position $\varphi(t)$ is displaced linearly with time. The angular velocity of the pendulum in this slow uniform motion equals the driving frequency: $\dot\varphi(t) = \omega$.

This means that we can assume a linear function $\varphi(t) \approx \omega t$ for the zero-order solution to equation (1) in the time interval $(-T/4, T/4)$. Similarly, for the adjacent interval $(T/4, 3T/4)$ we can write $\varphi(t) \approx \pi/2 - \omega(t - T/4) = \pi - \omega t$. As a whole, this approximate steady-state periodic solution is characterized by a saw-teeth pattern with equilateral triangle teeth. The simulation shows that this rectilinear tooth shape is slightly distorted near each apex by rapid oscillations occurring after the external torque reaches a maximum and the direction of motion of the equilibrium position is reversed. These rapid oscillations are especially pronounced in the angular velocity plot (figure 3). The angular velocity $\dot\varphi$ is expressed here in units ω_0 of the frequency of small undamped natural oscillations.

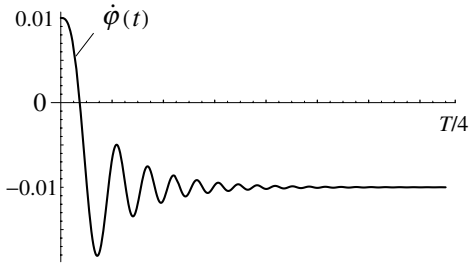

Figure 4. Approximate behaviour of the angular velocity at the low-frequency steady-state motion of the pendulum.

In order to investigate the character of these oscillations, we assume that the angle of deflection for the time interval $(T/4, 3T/4)$ can be expressed as $\varphi(t) \approx \pi - \omega t + \delta(t)$, where the correction $\delta(t)$ to the zero-order function is small: $\delta(t) \ll 1$. Differentiating equation (1) with respect to time, we obtain the following equation for the angular velocity $\dot{\varphi}(t) = \nu$:

$$\ddot{\nu} + 2\gamma\dot{\nu} + \omega_0^2 \cos\varphi(t)\nu = \omega\omega_0^2 \cos\omega t. \tag{2}$$

In the left-hand part of this equation, we can replace $\varphi(t)$ by its zero-order time dependence $\varphi(t) = \pi - \omega t$ and substitute for $\cos\varphi(t)$ its approximate expression $\cos(\pi - \omega t) = -\cos\omega t$. Thus instead of (2) we get an approximate second-order linear homogeneous equation for the angular velocity $\dot{\varphi}(t) = \nu$:

$$\ddot{\nu} + 2\gamma\dot{\nu} - \omega_0^2 \cos\omega t\,(\nu + \omega) = 0. \tag{3}$$

We can conclude from equation (3) that after the oscillations of the angular velocity ν damp out and ν approaches a constant value, so that its time derivatives in equation (3) become negligible; this constant value equals $-\omega$: $\dot{\varphi} = \nu \to -\omega$. During the preceding interval $(-T/4, T/4)$ oscillations of the angular velocity $\dot{\varphi}(t)$ have also damped out, and its constant value at the beginning of the interval $(T/4, 3T/4)$ approximately equals ω. Now it is convenient to transfer the time origin to the initial moment of the interval $(T/4, 3T/4)$, that is, to replace $t \to (t + T/4)$, or $\omega t \to (\omega t + \pi/2)$ in equation (3):

$$\ddot{\nu} + 2\gamma\dot{\nu} + \omega_0^2 \sin\omega t\,(\nu + \omega) = 0. \tag{4}$$

Oscillations of the angular velocity at the beginning of the interval $(T/4, 3T/4)$ are approximately described by a solution to this homogeneous equation. We note that in equation (4), $\sin\omega t$ can be replaced by ωt for the time interval we are interested in. Even after this simplification, equation (4) cannot be solved analytically. However, we can find numerically its particular solution for the given time interval with the help of any available mathematical package. The initial conditions for the starting point of this interval follow from the known pattern of the velocity graph for the periodic steady-state motion shown in figure 3: $\nu = \omega, \dot{\nu} = 0$. The graph in figure 4 shows the solution to equation (4) with these initial conditions obtained with the help of the 'Mathematica' package ($\omega = 0.01\omega_0$, $Q = \omega_0/2\gamma = 0.1$).

Comparing this graph with that shown in figure 3, we see that the approximate equation (4) indeed describes qualitatively the general character of the angular velocity oscillations occurring after the motion of the equilibrium position is reversed.

If amplitude ϕ_0 of the driving torque and its frequency are chosen to be a little greater than in the case considered above, the pendulum at first again follows the slowly varying torque

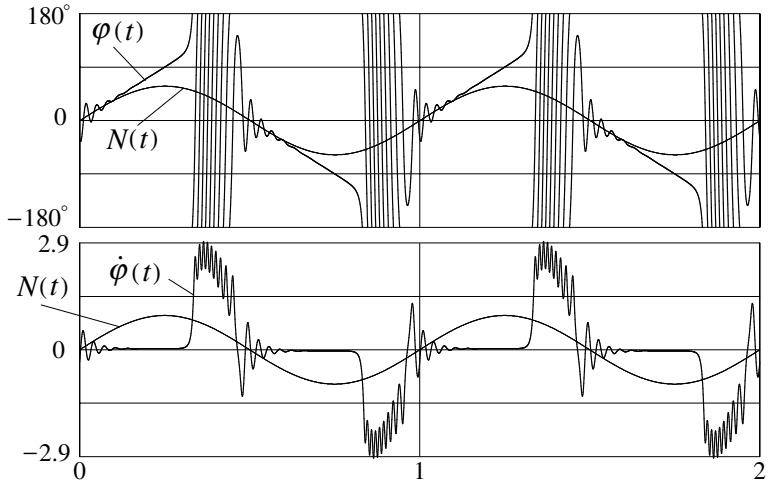

Figure 5. Rotations and oscillations of the pendulum under a slow-varying sinusoidal external torque.

so that the deflection angle $\varphi(t)$ also slowly increases almost linearly with time up to the highest (nearly horizontal) position. However, instead of reversing its slow motion alongside the equilibrium position when the latter starts to move back, the pendulum in this case escapes the shallow potential well over its low right barrier and 'slides down' along its bumpy outer slope (see curves 2 and 3 in figure 1). This means that the pendulum commences a rapid, unidirectional, nonuniform rotation. Figure 5 shows the graphs of the angular position $\varphi(t)$ and angular velocity $\dot{\varphi}(t)$ time dependence for this motion.

We can evaluate the average angular velocity $\langle\dot{\varphi}\rangle_{\rm av}$ of this rapid rotation by equating the external torque ϕ_0 at its maximum to the torque of viscous friction: $\omega_0^2\phi_0 = 2\gamma\langle\dot{\varphi}\rangle_{\rm av}$, whence $\langle\dot{\varphi}\rangle_{\rm av} \approx Q\omega_0$. The average period $T_{\rm rot}$ of this rotation can be estimated as $T_{\rm rot} = 2\pi/\langle\dot{\varphi}\rangle_{\rm av} \approx T_0/Q$, where $T_0 = 2\pi/\omega_0$ is the period of the small natural oscillations.

When t approaches $T/2$, the external torque $N(t)$ becomes smaller, the pendulum rotation gradually slows down and finally (when the torque almost vanishes) the pendulum becomes trapped in the potential well, within which it executes damped natural oscillations near the equilibrium position, which moves uniformly backward under the reversed external torque (see figure 5). Then all of the above-described motions repeat in the opposite direction.

4. Steady-state response–frequency curves of the pendulum

4.1. Approximate theoretical resonance curve, hysteresis and bistability

The steady-state response of a linear oscillator subjected to sinusoidal forcing is also a sinusoidal motion whose frequency equals the forcing frequency and whose amplitude depends on the frequency in a resonance manner. For the pendulum, as long as the driving amplitude is small and the damping is not too weak, the steady-state oscillation occurs with a small amplitude, so that the amplitude–frequency resonance curve is rather well approximated by the result for a harmonic oscillator.

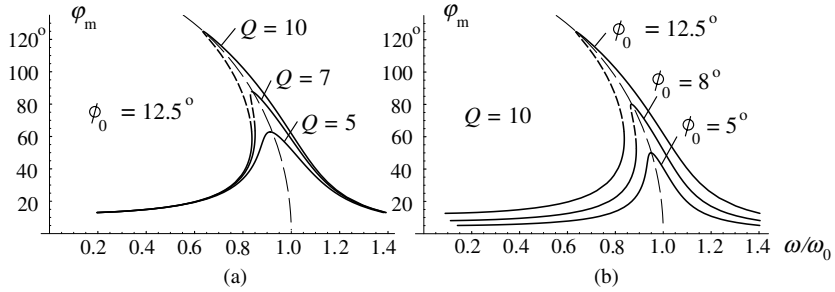

Figure 6. Approximate theoretical response–frequency curves of the pendulum: (a) constant driving amplitude $\phi_0 = 12.5^\circ$, (b) constant quality factor $Q = 10$.

For a stronger driving and/or weaker friction, the resonance curve of the pendulum bends towards lower frequencies and even folds, as is shown in figure 6. The nonlinear resonance curve can be approximated considerably well by the following heuristic approach [7]: we take the resonance curve of the harmonic oscillator and replace in it the natural frequency ω_0 by $\omega_{\mathrm{res}}(\varphi_{\mathrm{m}})$. This approach assumes that the steady-state oscillation is still harmonic, i.e. sinusoidal, but its frequency depends on the amplitude φ_{m}. For $\omega_{\mathrm{res}}(\varphi_{\mathrm{m}})$, we can use the approximate frequency–amplitude relation of the pendulum: $\omega_{\mathrm{res}} \approx \omega_0\big(1 - \varphi_{\mathrm{m}}^2/16\big)$ (the so-called skeleton curve shown by the thin dashed line in figure 6). The resonance peak at its maximum is shifted to lower frequencies and acquires a shape typical for nonlinear systems with a 'soft' restoring force. Over some critical value of the driving amplitude (for a given quality factor), the theoretical resonance curve becomes *S*-shaped with three solutions, only two of which are stable. This folding of the response–frequency curve leads to bistability and hysteresis.

Within some interval of driving frequencies, the pendulum oscillates with either a large amplitude or a small amplitude. In between there is always an unstable solution (see the left overhanging slope of resonance peaks shown by dashed lines in figure 6). Which of the two stable, periodic motions (limit cycles) is eventually established depends on the initial conditions.

A convenient traditional way to observe the nonlinear resonance response of the pendulum is to slowly vary ('sweep') the driving frequency from one side of the natural frequency through the resonance peak to the other side in a process of continuous steady-state oscillations, while the amplitude of the driving torque is kept constant. The pendulum responds differently depending on the direction of the frequency variation—there is an associated hysteresis characterized by abrupt jumps in the amplitude and phase of the steady-state response. When in the process of frequency sweeping an abrupt jump occurs from one slope of the folded resonance peak to the other, not only the amplitude of the steady-state oscillations changes considerably, but also the whole mode undergoes a dramatic change.

Figure 7 shows the response–frequency curve obtained with the help of the simulation program [6]. When we start the sweeping from low driving frequencies (and under the initial conditions of zero, with the pendulum resting in the equilibrium position), the observed steady-state response agrees perfectly well with the theoretical prediction: the forced oscillations occur almost in phase with the drive, and their amplitude grows gradually while the frequency is increased up to point *A*, which is characterized by a vertical tangent to the theoretical curve. Then an abrupt jump to point *B* lying on the right slope of the resonance peak occurs. After this jump, the amplitude and phase again agree well with the theoretical prediction. In the

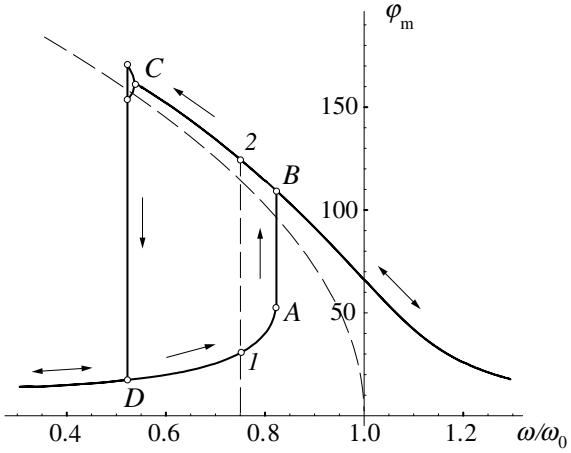

Figure 7. Hysteretic behaviour of the amplitude–frequency dependence during the up and down sweeping of the drive frequency ($\phi_0 = 12.5^\circ$, $Q = 10$).

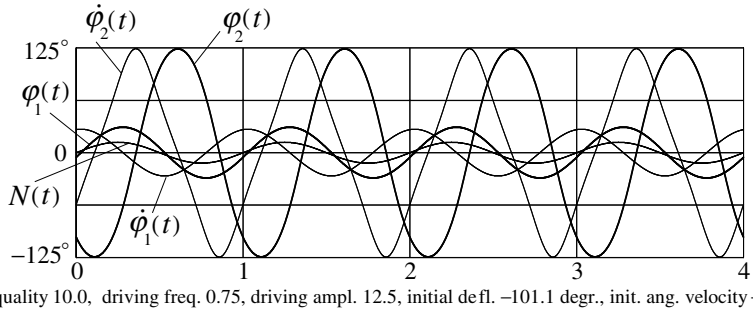

(quality 10.0, driving freq. 0.75, driving ampl. 12.5, initial defl. –101.1 degr., init. ang. velocity –0.92)

Figure 8. Graphs of the angle and angular velocity for small-amplitude (30°) and large-amplitude (125°) oscillations at the same parameters of the pendulum and of the external torque ($\omega = 0.75\omega_0$, $\phi_0 = 12.5^\circ$, and $Q = 10$). Initial conditions are indicated for the large-amplitude oscillations. These graphs correspond to points 1 and 2 respectively on the response-frequency diagram of figure 7.

process of further sweeping, the amplitude of the steady-state response gradually diminishes, and the pendulum oscillates in an almost opposite phase with respect to the driving torque.

If we reverse the direction of the frequency sweep, the pendulum's response on the way back follows the same curve up to point B. However, the amplitude, instead of jumping down, continues to increase along the right slope of the theoretical resonance peak after we have passed through point B. Figure 8 gives an example of this bistability. Indeed, during the direct sweeping from left to right the steady-state oscillations at point 1 are almost sinusoidal in shape (curves $\varphi_1(t)$ and $\dot\varphi_1(t)$ in figure 8) and occur nearly in the same phase with the driving torque $N(t)$, while on the way back, at point 2 (at the same frequency and amplitude of the drive as at point 1), the oscillations have a much greater amplitude and lag in phase behind the torque more than a quarter period. These oscillations are no longer harmonic: the graph of $\dot\varphi_2(t)$ has a saw-toothed appearance, while the graph of $\varphi_2(t)$, though resembling a sinusoid, actually consists of nearly parabolic alternating segments.

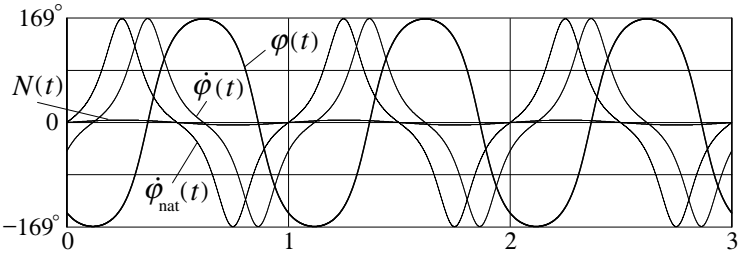

(quality 30.0, driving freq. 0.442, driving ampl. 4.0, initial defl. −147.0 degr., init. ang. velocity −0.555)

Figure 9. Graphs of $\varphi(t)$ and $\dot{\varphi}(t)$ for the bell-ringer mode of forced oscillations. The graph of $\dot{\varphi}_{\rm nat}(t)$ for natural undamped oscillations ($\phi_0 = 0$) of the same amplitude (about 168°) is also shown.

Steady-state modes $\varphi_1(t)$ and $\varphi_2(t)$, coexisting at the same frequency and amplitude of the drive, differ in amplitude and in phase relationships with the driving torque—they correspond to different slopes of the resonance peak. The large-amplitude mode $\varphi_2(t)$ has a much smaller basin of attraction than $\varphi_1(t)$.

4.2. Nonlinear resonance and a 'bell-ringer mode'

As one sweeps the drive frequency towards lower values, one moves to the left in figure 7 almost along the skeleton curve and can reach amplitudes that are considerably greater than the estimated theoretical maximum (see figure 6). For weak damping, the steady-state amplitude at low drive frequencies can be very large (approaching 180°) at moderate and even quite small drive amplitudes. Traces in figure 9 give an example of such extraordinary motion of the pendulum, which was called by Peters [8] a 'bell-ringer mode.' In this mode the pendulum passes rapidly through the lower equilibrium position, but 'sticks' near the extreme points of oscillation, spending a very long time moving slowly in the vicinity of an unstable equilibrium position (near the saddle point in the phase plane).

These large-amplitude oscillations give an example of nonlinear resonance: their period (which equals the drive period) is very close to the period of natural oscillations of the same amplitude. For large amplitudes, this period can last several periods of small natural oscillations. Actually, such forced oscillations under conditions of nonlinear resonance are very much like natural oscillations that occur at the corresponding large amplitude. To emphasize this similarity, we show in figure 9, together with the graph of $\dot{\varphi}(t)$, also the graph of $\dot{\varphi}_{\rm nat}(t)$ for natural undamped oscillations ($\phi_0 = 0$) of the same amplitude (about 168°).

We can exploit the similarity between the bell-ringer mode and natural undamped oscillations for theoretical calculation of the amplitude at a given resonant drive frequency. It was shown in [1] that for non-sinusoidal natural oscillations with an amplitude $\varphi_{\rm m}$ approaching 180°, the period depends on the amplitude as follows:

$$T = \frac{2}{\pi} T_0 \ln \frac{8}{\pi - \varphi_{\rm m}}, \qquad \text{whence} \qquad \varphi_{\rm m} = \pi - 8 \exp\left(-\frac{\pi}{2}\frac{\omega}{\omega_0}\right). \tag{5}$$

In the simulation presented in figure 9, the frequency of the drive $\omega = 0.442\omega_0$. Substituting this value in equation (5), we find for the corresponding amplitude of undamped natural oscillations: $\varphi_{\rm m} = 167°$. This theoretical estimate is very close to the amplitude of the bell-ringer forced oscillations ($\varphi_{\rm m} \approx 168°$) observed in the simulation experiment at the drive frequency $\omega = 0.442\omega_0$.

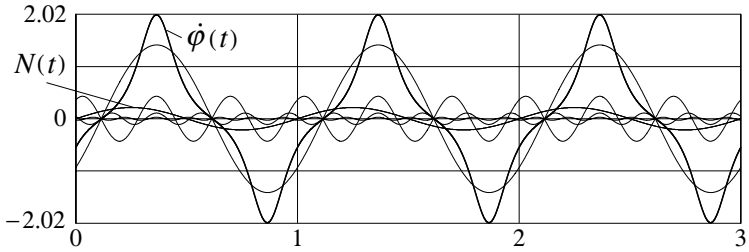

(quality 30.0, driving freq. 0.442, driving ampl. 4.0, initial defl. −147.0 degr., init. ang. velocity −0.555)

Figure 10. Graphs of angular velocity $\dot{\varphi}(t)$ and its harmonics for the bell-ringer mode of forced oscillations.

When the drive period is almost equal to the period of large natural oscillations, full synchronization between the motions (phase locking) can occur. The pendulum lags in phase about a quarter period behind the periodic external torque $N(t)$. Due to the phase locking, this small torque $N(t)$ at resonance is almost always directed in phase with the angular velocity $\dot{\varphi}(t)$ of the pendulum (see figure 10) and therefore supplies the pendulum with energy needed to compensate for frictional losses and to maintain the constant amplitude of large non-sinusoidal nearly natural oscillations.

An alternative physical explanation of the bell-ringer mode is based on considering the motion of a particle in a time-dependent spatially periodic potential (see curve 1 in figure 1) whose pattern is 'rocking' slightly about the origin (point 0), so that the right barrier of the well lowers a bit and the left one rises when the external torque is directed to the right, and vice versa, after a half-period of the drive. Let us imagine that the particle in the well on its way from left to right slowly 'climbs up' the slope of the right barrier and turns back approximately at the time when the potential pattern is horizontal (zero external torque), and passes back through the bottom of the well just after the moment at which the right barrier is at its maximal height. The duration of the particle motion back and forth in the non-parabolic well depends on the amplitude, and if this duration equals the period of 'rocking' of the potential pattern, phase locking can occur and a steady-state process can eventually establish. The energy needed to overcome friction is supplied by the source that 'rocks' the potential pattern (that is, by the periodic external torque).

This bell-ringer mode can certainly also be excited by carefully choosing proper starting conditions. However, to maintain the large-amplitude motion, the phase relation between the pendulum and the drive torque is critical. This means that for this mode the basin of attraction on the phase plane of initial conditions is rather small. Hence, it is much easier to reach this mode experimentally by sweeping down the drive frequency as described above. After each step along the way, we must wait for the transients to settle.

The spectrum of the bell-ringer large-amplitude oscillations, besides the fundamental harmonic whose period equals the driving period, also contains several harmonic components of higher orders. Their frequencies are odd integer multiples of the fundamental frequency. Figure 10 shows the graphs of angular velocity $\dot{\varphi}(t)$ and its harmonics for the bell-ringer mode.

4.3. Symmetry-breaking and period-doubling bifurcations, chaos and crisis

A further decrease of the drive frequency brings the system to point C (see figure 7) at which a symmetry-breaking bifurcation occurs: the pendulum's excursion to one side is greater

than to the other side, for example 173° versus 165°. This spatial asymmetry of oscillations increases as we move further to lower frequencies. In the spectrum of such asymmetric steady-state oscillations, besides harmonics of odd orders, even-order harmonics of small amplitudes are present, including a zero-order component (constant mid-point displacement). Such asymmetric modes exist in pairs whose phase orbits (at the same drive frequency) are the mirror images of one another.

In this way, at a certain frequency, a period-doubling bifurcation occurs: in each subsequent cycle the maximal deflection to the same side slightly differs from the preceding one, but after two cycles the motion repeats exactly. This means that the period of this steady-state oscillation equals two drive periods. Period doubling breaks the original time-translational symmetry of the sinusoidally driven pendulum: although the driving torque repeats exactly from cycle to cycle, the pendulum executes slightly different motions on alternate cycles. For this motion, the Poincaré section consists of two nearby points in the phase plane visited in alternation.

What happens after this period-doubling bifurcation in the simulation experiment depends strongly on details of the frequency diminution. If the sweeping occurs in very small steps, a whole cascade of close-set period-doubling bifurcations can be observed. Each bifurcation in this series doubles the period of motion and the number of fixed points in its Poincaré map.

This cascade of period-doubling bifurcations converges to a chaotic large-amplitude oscillation of the pendulum. During these chaotic oscillations of the bell-ringer type, the maximal deflection is close to 180° and varies randomly from cycle to cycle whose duration equals approximately one driving period. In contrast to a complicated initial transient that eventually leads to a regular motion characterized by a fixed finite set of Poincaré sections, this chaotic regime persists indefinitely. The Poincaré map consists of two small nearby islands visited in alternation. Within each island, the point bounces randomly from cycle to cycle. This chaotic state is stable in the sense that after a small perturbation, the phase trajectory converges to the same region. Attracting regions in the phase space that correspond to chaotic regimes are called strange attractors because they are formed by fractals—geometric objects of non-integer dimensions. The fractal character of attractors is essential to the existence of persistent dynamical chaos.

The chaotic oscillatory regime following the bell-ringer mode exists in a very narrow interval of the driving frequencies, so that a slight perturbation can cause a crisis leading to an abrupt jump of the amplitude down to point D (see figure 7) located on the far left outskirt of the resonance peak. If the frequency sweeping is executed by steps that are not small enough, this jump can occur before the chaotic regime is established or even before the period-doubling bifurcation occurs.

Actually, this abrupt jump of the amplitude is presented by a long irregular transient during which the motion of the pendulum undergoes a radical rearrangement. Details of this transient are very sensitive to the character of perturbation (to the magnitude and timing of the frequency step). In particular, the initial stage of the transient may have the character of intermittency: during a long time the pendulum executes an asymmetric oscillation in which its excursion, say, to the left side is greater than to the right side. Then during several cycles the asymmetry changes to the opposite, that is, to prolonged oscillations with a greater maximal deflection to the right side. Such irregular interchanges of the two spatially asymmetric regimes are characterized by a time scale much longer than the cycle duration (the drive period), and can occur several times before the crisis.

The crisis leading to the jump down of the amplitude can be initiated, for example if irregular amplitude variations lead the pendulum to cross the vertical (to make a full revolution), after which the pendulum gradually settles down to the low-frequency and low-amplitude

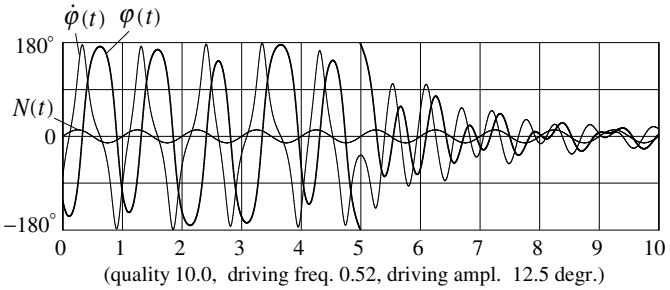

Figure 11. Transition from large-amplitude nonlinear oscillations (from the irregular bell-ringer mode) to small-amplitude ordinary forced oscillations.

regular (sinusoidal) steady-state oscillation for which the angular displacement $\varphi(t)$ almost exactly equals the driving torque: $\varphi(t) \approx \phi_0 \sin \omega t$. The simulation of motion in figure 11 shows us what can happen during a transient that accompanies this amplitude jump.

If after this jump down of the amplitude at point D (see figure 7) we continue to sweep down the frequency, the amplitude and phase of steady-state oscillations again obey the theoretical response–frequency curve, just as they did while sweeping the frequency from left to right.

5. Subharmonic and superharmonic resonances

Steady-state forced oscillations of a large amplitude, resembling the bell-ringer mode, can also occur if the driving frequency is approximately three times greater than the natural frequency that corresponds to this large amplitude. Figure 12 clearly shows that the third harmonic of these steady-state oscillations has the frequency that equals the driving frequency, while the frequency of the fundamental harmonic equals one-third of the driving frequency. In other words, one cycle of such non-harmonic oscillations of the pendulum covers three driving periods. Forced period-3 oscillations of large amplitude occurring under such conditions give an example of nonlinear third-order subharmonic resonance. Subharmonic resonances do not exist in linear systems.

Similar to the bell-ringer mode (see figure 10), the pendulum behaves here very much like during free oscillations. The sinusoidal external torque, being synchronized with the third harmonic of these non-harmonic large-amplitude natural oscillations, compensates for frictional losses and maintains a constant angular excursion. This synchronization (phase locking) can occur only if at $t = 0$ (the time moment when the torque is switched on) large-amplitude natural oscillations already exist. This means that for a given frequency of the external torque (lying within a definite interval), the third-order subharmonic resonance occurs only for initial conditions from a certain region (from the basin of attraction of this limit cycle). Different initial conditions cause the pendulum to eventually settle down into the low-amplitude period-1 anti-phase oscillation that corresponds to the far-off high-frequency slope of the nonlinear resonance peak.

During slow reduction of the driving frequency under conditions of the third-order subharmonic resonance, a symmetry-breaking bifurcation occurs, after which the angular excursion to one side is greater than to the opposite side. Such spatially asymmetric modes exist in pairs whose phase orbits are the mirror images of one another. Further reduction of the driving frequency leads to a crisis: after a long transient the pendulum settles into

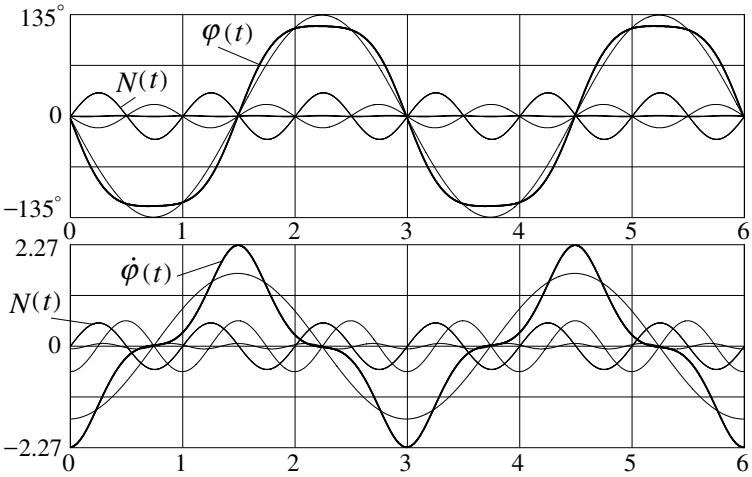

(quality 280.0, driving freq. 1.85, driving ampl. 35.0, initial defl. −3.99 degr., init. ang. velocity −2.27)

Figure 12. Subharmonic resonance of the third order.

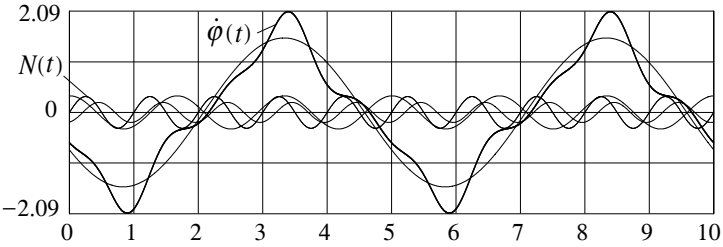

(quality 100.0, driving freq. 2.65, driving ampl. 26.18, initial defl. 142.95 degr., init. ang. velocity –0.6272)

Figure 13. Graphs of angular velocity $\dot{\varphi}(t)$ and its harmonics at subharmonic resonance of the fifth order.

the ordinary anti-phase mode of forced oscillations that correspond to the right slope of the nonlinear resonance curve.

At subharmonic resonance of the fifth order (see the graph of $\dot{\varphi}(t)$ and its harmonics in figure 13), one cycle of the pendulum's almost natural oscillation covers five driving periods: the external torque is synchronized with the fifth harmonic of a period-5 large-amplitude oscillation of the pendulum. On average, this phase locking provides a surplus of energy transferred to the pendulum over the energy returned back to the source of the external torque, thus compensating for frictional losses.

Gradually reducing the driving frequency under conditions of the fifth-order subharmonic resonance, we can observe the symmetry-breaking and period-tripling bifurcations, after which the period of steady-state forced oscillations equals 15 driving periods. The set of Poincaré sections consists of 15 fixed points in five groups visited by turn. Each group consists of three nearby points.

The subharmonic resonances discussed above occur at rather high drive frequencies, which are equal to an odd integer of the natural frequency. In contrast, superharmonic resonances can be excited at rather low drive frequencies: synchronization of the drive with oscillations of

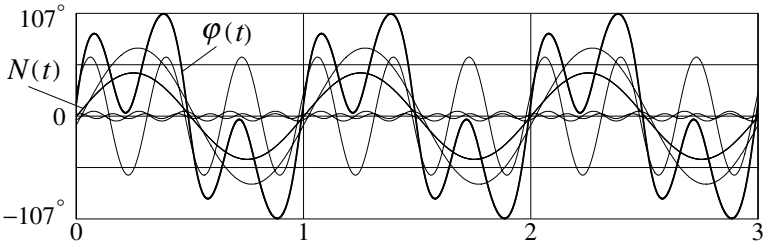

(quality 25.0, driving freq. 0.26, driving ampl. 45.0, initial defl. 13.28 degr., init. ang. velocity 1.253)

Figure 14. Plots of angular deflection $\varphi(t)$ and its harmonics at superharmonic resonance of the third order occurring under the sinusoidal external torque $N(t)$.

the pendulum (phase locking) occurs if one period of the drive covers an odd integer number of natural periods.

The nature and origin of superharmonic resonances can be explained in the following way. Let us consider natural nonlinear oscillations of the pendulum in a potential well that slowly moves back and forth due to sinusoidally varying (with driving frequency ω) external torque. Under certain conditions, an integer number of natural cycles covers one period of the potential well motion. Figure 14 clearly shows that for the third-order superharmonic resonance, just three natural cycles are executed during one period of the drive. In this case, phase locking of the potential well motion with natural oscillations can occur. By virtue of this synchronization, the external torque can continuously supply the pendulum with energy required to compensate for frictional losses and prevent damping of short-period natural oscillations of the pendulum in the moving potential well. As a result, a steady-state non-sinusoidal period-1 oscillation (its period equals that of the drive) is established, whose spectrum is distinguished by the considerable contribution of the third harmonic.

Depiction of such a motion on the computer screen with the help of the simulation program [6] allows us to develop an intuitive feel for how nonlinear systems generate high harmonics of the sinusoidal input oscillation. The simulation tells us much more for understanding this phenomenon than the mathematical equations.

Superharmonic resonances are also accompanied by symmetry-breaking bifurcations and chaotic regimes. Examples of strange attractors that follow superharmonic resonances of the third and fifth orders are shown in figures 15(a) and (b), respectively.

6. Other extraordinary regular forced oscillations

The original time-translational symmetry in the motion of the sinusoidally driven pendulum can be broken not only by the above-described period-doubling bifurcations: under certain conditions regular oscillations of the pendulum have a period which covers some integer (other than two) number of the drive period.

Figure 16 shows the graphs of $\varphi(t)$ and $\dot{\varphi}(t)$ with harmonics for a period-3 nonlinear oscillation in which the frequency of the third harmonic coincides with the driving frequency. The pendulum makes one oscillation during each drive period, but the swing differs from one cycle to the next as though the mid-point were moving with a period that is three times the drive period: maximal angular excursion of the pendulum equals 171°, then 117° and then 111°. After three cycles of the external torque, all the motion repeats. The set of Poincaré sections consists of three fixed points visited in turn. If the initial conditions are chosen somewhere

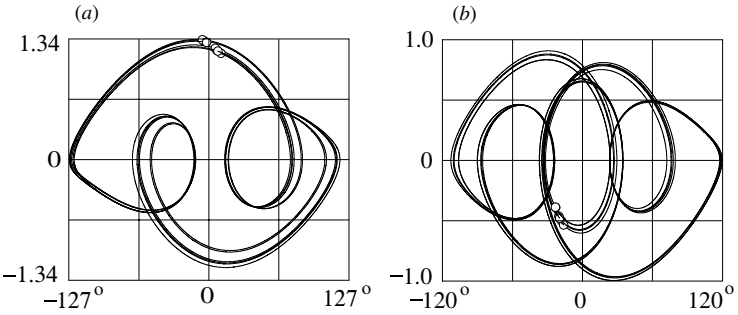

a—quality 7.1, driving freq. 0.23, driving ampl. 51.0, initial defl. 7.45 degr., init. ang. velocity 1.22
b—quality 22.0, driving freq. 0.1483, driving ampl. 50.0, initial defl. −17.95 degr., init. ang. velocity −0.50

Figure 15. Phase diagrams (with Poincaré sections) of chaotic oscillations in the vicinity of superharmonic resonances of the third (a) and fifth (b) orders.

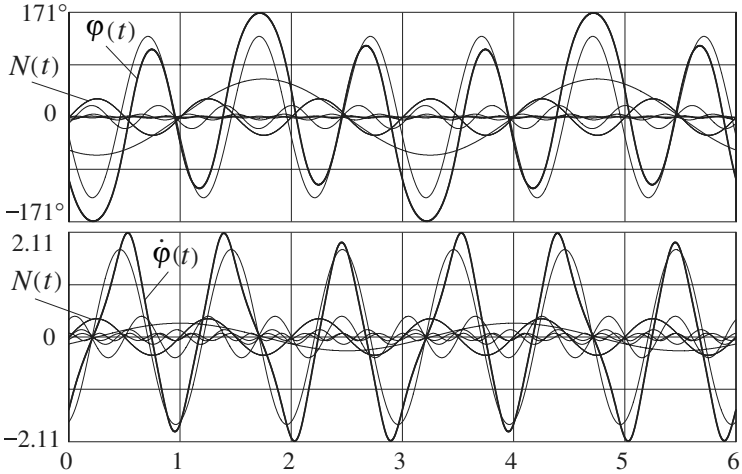

(quality 15.0, driving freq. 0.765, driving ampl. 30.0, initial defl. 43.48 degr., init. ang. velocity −2.037)

Figure 16. Period-3 nonlinear oscillations. The frequency of the fundamental harmonic equals one-third of the driving frequency.

beyond the basin of attraction of this mode, the pendulum eventually settles into a coexisting simple mode—period-1 spatially symmetric oscillations with an amplitude of 142° that occur in the opposite phase with respect to the driving torque.

When the driving frequency is slightly smaller than the natural frequency, rather counterintuitive steady-state modes can occur in which the motion of the pendulum resembles beats: the amplitude and frequency of oscillation are not constant but instead vary slowly with a long period that equals an integer (odd and rather large) number of driving periods. An example of such modulated steady-state oscillations whose period equals eleven driving cycles is shown in figure 17. We note the most surprising feature of this mode: the maximal deflections of the pendulum have no tendency to equalize in the course of time. In contrast to ordinary transient beats, in these oscillations the variations of amplitude and frequency do not fade: once established, they continue forever.

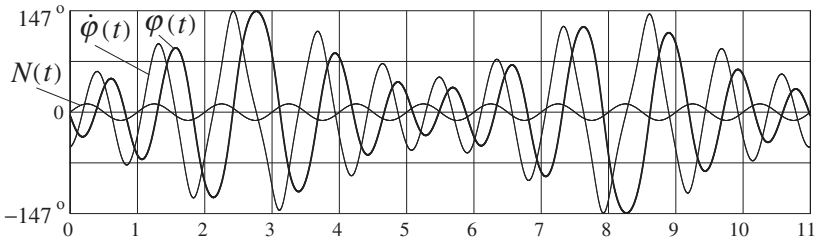

(quality 600.0, driving freq. 0.9, driving ampl. 12.0, initial defl. −5.18 degr., init. ang. velocity −0.677)

Figure 17. Period-11 forced steady-state oscillations.

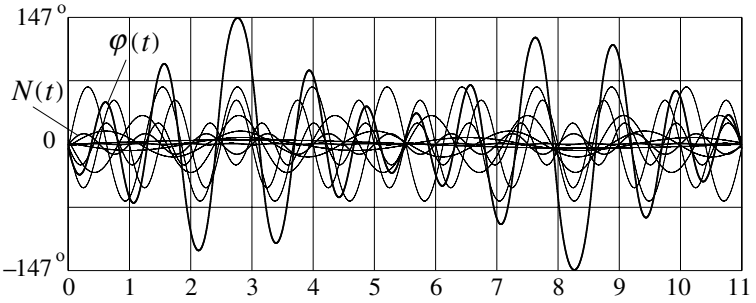

(quality 600.0, driving freq. 0.9, driving ampl. 12.0, initial defl. −5.18 degr., init. ang. velocity −0.677)

Figure 18. Harmonic components (the spectrum) of period-11 forced oscillations.

We can suggest a simple physical explanation for this exotic mode. Let the phase of the sinusoidal driving torque be initially almost equal to the phase of (natural) oscillations of the angular velocity. That is, let us assume that the external torque varies with time in such a way that it is directed along the angular velocity during almost the entire period. In this case, the energy is transferred to the pendulum and the amplitude of oscillations gradually grows. But with the growing amplitude, the natural period of the pendulum becomes longer. Therefore after a while the oscillations of the angular velocity accumulate some phase lag with respect to the driving torque. When this phase lag increases up to 180°, that is, the driving torque varies in the opposite phase with respect to the angular velocity, the energy flow is reversed. This causes the swing of oscillations to decrease.

Then after a while the phase relations again become favourable for supplying the energy to the pendulum, and the amplitude grows again. Thus, the amplitude of oscillations is modulated with some (rather long) period. A small amount of friction can stabilize the period of modulation. If this period equals an integer number of the driving periods, the phase locking can occur. By virtue of this synchronization between the drive and natural oscillations, the whole process of modulated oscillations becomes exactly periodic. The energy dissipation is compensated by a somewhat greater amount of energy being transferred to the pendulum on average (during a cycle of the modulation) compared to the backward transfer from the pendulum to the source of the external drive.

Thin lines in figure 18 show harmonic components (the spectrum) of these period-11 oscillations. The fundamental harmonic of this non-sinusoidal oscillation has 1/11th of the

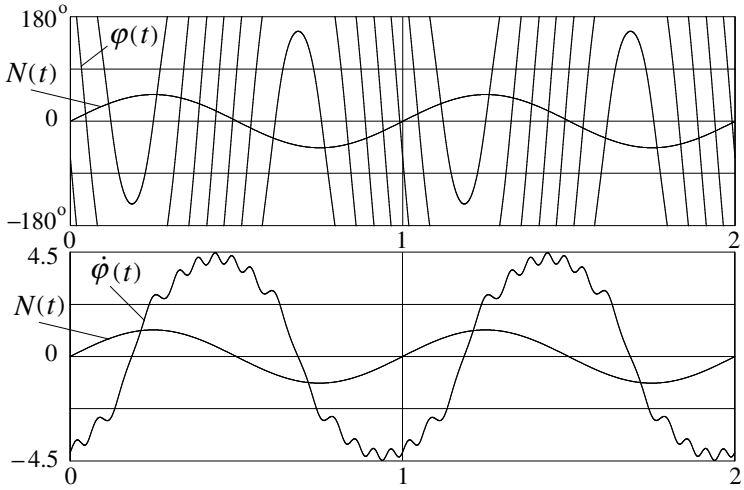

(quality 15.0, driving freq. 0.22, driving ampl. 45.8, initial defl. −63.36 degr., init. ang. velocity −4.183)

Figure 19. Stationary period-1 fast bidirectional revolutions of the pendulum.

Table 1. Amplitudes of odd harmonics for period-11 oscillations.

No	Amplitude (radians)	Amplitude (degrees)	Velocity (units of ω_0)
1	0.091	5.214	0.007
3	0.137	7.850	0.039
5	0.269	15.41	0.121
7	0.585	33.52	0.374
9	1.164	66.69	0.951
11	0.883	50.59	0.885
13	0.428	24.52	0.507
15	0.013	0.745	0.018

driving frequency ω. Its amplitude is an order of magnitude smaller than the amplitude of the 11th harmonic component whose frequency equals the driving frequency. Besides this component, harmonics with frequencies $7/11$, $9/11$ and $13/11$ of the driving frequency contribute considerably to the resulting oscillation. The amplitudes of odd harmonics are listed in table 1.

Another example of a periodic steady-state forced motion of a pendulum is presented in figure 19. During one period of the external torque, the pendulum makes six fast revolutions to one side; then its rotation slows down and it makes six revolutions to the opposite side.

From the angular velocity graph, we suppose that the time dependence of $\dot{\varphi}(t)$ can be represented as a superposition of a slow periodic component (varying almost sinusoidally with the drive period T) and a small fast component distorting this slow variation. We suppose that the slow variation of $\dot{\varphi}(t)$ is caused by the slow varying external torque, while the additional fast oscillations of $\dot{\varphi}(t)$ appear by virtue of the gravitational force that influences the pendulum rotation. Hence to a first approximation, this extraordinary behaviour of the pendulum can be explained by neglecting the force of gravity. Omitting the last term in the left-hand

part of equation (1), we get the following linear first-order equation for the angular velocity $\nu(t) = \dot{\varphi}(t)$:

$$\dot{\nu} + 2\gamma\nu = \omega_0^2\phi_0 \sin\omega t. \tag{6}$$

The steady-state periodic solution of this equation can be represented as follows:

$$\nu(t) = -\nu_m \cos(\omega t + \delta), \qquad \nu_m = \frac{\omega_0^2\phi_0}{\sqrt{\omega^2 + 4\gamma^2}}, \qquad \delta = \arctan\frac{2\gamma}{\omega}. \tag{7}$$

Hence, the angular velocity $\nu(t)$ varies sinusoidally with the drive frequency ω and the amplitude ν_m given by equation (7). Actually, $\nu(t)$ corresponds to the slow component of $\dot{\varphi}(t)$ averaged over the period of fast rotation: $\nu(t) = \langle\dot{\varphi}(t)\rangle_{av}$. According to equation (7), its amplitude $\nu_m \approx \omega_0^2\phi_0/\omega$ equals $3.6\omega_0$ for the values $\phi_0 = 0.8$ and $\omega = 0.22\omega_0$ that were used in the simulation experiment shown in figure 19, while the phase lag $\delta = \arctan(2\gamma/\omega) = \arctan(\omega_0/Q\omega) \approx 0.3$. These values agree rather well with the experiment. To evaluate the minimal period Δt of fast rotation, we can divide the full angle 2π by the average angular velocity ν_m, whence $\Delta t/T = \omega/\nu_m = 0.06$, which also agrees well with the experimental graph in figure 19.

We can evaluate the amplitude of fast oscillations of the angular velocity $\dot{\varphi}(t)$ on the basis of the energy conservation. Let $\dot{\varphi}_{max}$ and $\dot{\varphi}_{min}$ be the maximum and minimum values of $\dot{\varphi}(t)$ during the stage of fastest rotation. The kinetic energy of the rotating pendulum at the lowest point (which is proportional to $\dot{\varphi}_{max}^2$) is greater than at the inverted position approximately by the difference in the potential energy at these points. From these considerations, we find

$$\dot{\varphi}_{max,min} = \nu_m\left(1 \pm \frac{\omega_0^2}{\nu_m^2}\right), \qquad \nu_m = \frac{\omega_0^2\phi_0}{\sqrt{\omega^2 + 4\gamma^2}} \approx \frac{\omega_0^2\phi_0}{\omega}. \tag{8}$$

According to this estimate, the fractional difference $(\dot{\varphi}_{max} - \dot{\varphi}_{min})/\nu_m$ at $\phi_0 = 0.8$ and $\omega = 0.22\omega_0$ equals 0.15, again in a good agreement with the experiment.

An alternative physical explanation of this mode may be formulated by considering the motion of a particle in a time-dependent periodic potential (see curve 1 in figure 1) whose lateral barriers are slowly rising and falling with time. In contrast to the similar approach in the explanation of the bell-ringer mode (see section 4.2), now the potential pattern is 'rocking' about the origin (point 0) with a large amplitude. After escaping the potential well by crossing its falling barrier, the particle starts to slide down along the bumpy slope crossing the barriers until the next barrier rises high enough to slow down the particle and to force its backward non-uniform motion.

To maintain this exotic steady-state periodic motion (to provide the phase locking), the phase relation between the pendulum and the periodic variation of the potential pattern (that is, the drive torque $N(t)$ time dependence) is critical. This means that the mode can be excited only by choosing the initial conditions carefully. In other words, this limit cycle is characterized by a small basin of attraction.

7. Concluding remarks

The dynamic behaviour of the planar forced pendulum discussed in this paper is richer in various modes than we might expect for such a simple physical system relying on our intuition. Its nonlinear large-amplitude motions can hardly be called simple. Variations of the parameters result in different regular and chaotic types of dynamical behaviour. The program 'rigid pendulum driven by a sinusoidal torque' [6] offers many interesting predefined examples (besides those discussed above) that illustrate various peculiarities of this famous

physical model in vivid computer simulations. Visualization of the motion simultaneously with plotting the graphs of different variables and phase trajectories makes the simulation experiments very convincing and comprehensible.

In this paper, we have touched on only a small portion of the steady-state modes and regular motions of the sinusoidally driven rigid pendulum. The pendulum's dynamics exhibit a great variety of other counterintuitive rotational, oscillatory and combined (both rotational and oscillatory) multiple-periodic stationary states (attractors), whose basins of attraction are sometimes characterized by a surprisingly complex (fractal) structure. Computer simulations also reveal intricate sequences of bifurcations, leading to numerous intriguing chaotic regimes. Most of these features remain beyond the scope of this paper. With good reason we can say that this familiar and apparently simple physical system seems almost inexhaustible.

References

[1] Butikov E I 1999 The rigid pendulum—an antique but evergreen physical model *Eur. J. Phys.* **20** 429–41
[2] Baker G L and Gollub J P 1990 *Chaotic Dynamics. An Introduction* (Cambridge: Cambridge University Press)
[3] Miles J W 1988 Resonance and symmetry breaking for the pendulum *Physica* D **31** 252–68
[4] Heng H, Doerner R, Hübinger B and Martienssen W 1994 Approaching nonlinear dynamics by studying the motion of a pendulum: I. Observing trajectories in phase space *Int. J. Bifurcation Chaos* **4** 751–60
[5] Doerner R, Hübinger B, Heng H and Martienssen W 1994 Approaching nonlinear dynamics by studying the motion of a pendulum: II. Analyzing chaotic motion *Int. J. Bifurcation Chaos* **4** 761–71
[6] Butikov E I 2004 *Rigid Pendulum Driven by a Sinusoidal Force* (the simulation program) http://www.ifmo.ru/butikov/Nonlinear
[7] Landau L D and Lifschitz E M 1988 *Mechanics* (Moscow: Nauka) (in Russian)
Landau L D and Lifschitz E M 1976 *Mechanics* (New York: Pergamon)
[8] Peters R D 1996 Resonance response of a moderately driven rigid planar pendulum *Am. J. Phys.* **64** 170–3